NANO · MICRO small
www.small-journal.com

SARS-CoV-2 Spike Stem Protein Nanoparticles Elicited Broad ADCC and Robust Neutralization against Variants in Mice

*Yao Ma, Ye Wang, Chunhong Dong, Gilbert X. Gonzalez, Wandi Zhu, Joo Kim, Lai Wei, Sang-Moo Kang, and Bao-Zhong Wang**

Severe acute respiratory syndrome coronavirus 2 (SARS-CoV-2) has caused the global pandemic. The virus is rapidly evolving, characterized by the emergence of several major variants. Stable prefusion spike protein (Pre) is the immunogen in current vaccines but is limited in protecting against different variants. Here, the immune responses induced by the relatively conserved stem subunit (S2) of spike protein versus Pre are investigated. Pre generates the most robust neutralization responses against SARS-CoV-2 variants in vesicular stomatitis virus pseudovirus-based assessment but elicits less antibody-dependent cellular cytotoxicity (ADCC) activity than S2. By contrast, S2 induces the most balanced immunoglobulin G (IgG) antibodies with potent and broad ADCC activity although produces weaker neutralization. The immunogenicity of S2 and Pre improves by incorporating the two proteins into double-layered protein nanoparticles. The resulting protein nanoparticles Pre/S2 elicit higher neutralizing antibodies than Pre alone, and stronger ADCC than S2 alone. Moreover, nanoparticles produce more potent and balanced serum IgG antibodies than the corresponding soluble protein mixture, and the immune responses are sustained for at least four months after the immunization. Thus, the double-layered protein nanoparticles have the potential to be developed into broader SARS-CoV-2 vaccines with excellent safety profiles.

1. Introduction

Since later 2019, the severe acute respiratory syndrome coronavirus 2 (SARS-CoV-2) pandemic has caused more than 5.7 million death and continues to be a public health burden worldwide.[1,2] Vaccination is the most effective strategy to end the pandemic. However, the continued emergence of variants and the resulting increases in breakthrough infections compromise the protective efficacy of current vaccines based on the original virus strain.

Since the initial SARS-CoV-2 reported in China, multiple variants have emerged worldwide.[2,3] Notably, B.1.1.7 (Alpha, α) was first detected in September 2020 in southeast England and has shown enhanced transmissibility and increased mortality compared with the original lineage.[4,5] Moreover, B.1.351 (Beta, β) and P.1 (Gamma, γ) variants were first identified in South Africa and Brazil, respectively, and partially circumvented postinfection or vaccination immunity.[6–15] Subsequently, the novel B.1.617.2 (Delta, δ) variant that emerged in India spread quickly across the globe,[16–19] as it displayed increased transmissibility beyond B.1.1.7 and enhanced vaccine evasion like B.1.351.[20–26] The most heavily mutated variant so far identified in Botswana and named as B.1.1.529 (Omicron, o), is rapidly becoming the dominant SARS-CoV-2 virus circulating globally and joins the World Health Organization (WHO) list of variants of concern with Delta, Alpha, Beta, and Gamma.[27,28] Such variants with striking antibody evasion and rapid transmission even in fully vaccinated individuals present a critical threat to pandemic control and disease treatment.[29–35]

The spike protein (S) is the preferred target antigen for vaccine development, based on its essential function and abundant neutralizing epitopes.[36] S is a class I virus fusion protein including S1 and S2 subunits connected by a furin-like cleavage site.[37,38] With the receptor-binding domain (RBD), S1 recognizes and anchors the angiotensin-converting enzyme 2 (ACE2) on the host cellular membrane during viral infection. The fusion peptide (FP) in the S2 subunit mediates the fusion of the viral membrane with the cell membrane.[39–42] Based on the RBD and FP functions, S is transformed from the metastable prefusion conformation to the stable postfusion conformation during the S-protein-mediated viral cell entry through structural rearrangement.[43]

Due to its integral role in infection, current messenger RNA (mRNA) and nonreplicating viral vector vaccines have used the stabilized prefusion conformation of S protein (Pre) as the major antigen to induce potent humoral and cellular immune responses.[39,44–48] However, S-based vaccines face challenges as mutations continue to emerge. Most mutations occur on the relatively variable S1 subunit, the main target of vaccine-induced neutralizing antibodies. For instance, the D614G mutation exhibits enhanced replication and transmission during viral spread and has supplanted the ancestral virus and appears

Y. Ma, Y. Wang, C. Dong, G. X. Gonzalez, W. Zhu, J. Kim, L. Wei, S.-M. Kang, B.-Z. Wang
Center for Inflammation Immunity & Infection
Institute for Biomedical Sciences
Georgia State University
Atlanta, GA 30302, USA
E-mail: bwang23@gsu.edu

The ORCID identification number(s) for the author(s) of this article can be found under https://doi.org/10.1002/smll.202200836.

DOI: 10.1002/smll.202200836

in nearly all current variants. Furthermore, N501Y has appeared in the Alpha, Beta, Gamma, Theta (P3, θ), Mu (B.1.621, μ), and Omicron variants' RBD domain, increasing ACE2 affinity and virus replication.[49–51] In addition, some other RBD mutations like K417N/T (appeared in Beta, Gamma, and Delta sublineages AY.1 and AY.2 variants), L452R (appeared in Epsilon, Kappa, and Delta variants), and E484K (appeared in Beta, Gamma, Zeta, Theta, Eta, and Mu variants) show reduced susceptibility to current RBD monoclonal antibodies.[6,18,52–59]

In contrast to S1, the membrane-proximal S2 stem subunit is more conserved during evolution. Correspondingly, some S2-specific human antibodies have effectively neutralized a broad panel of beta-coronaviruses.[60–63] Previous research has identified a linear peptide in S2 as a potential vaccine candidate for comprehensive protection against SARS-CoV-2 and variants.[64] Therefore, S2 is a promising target for a SARS-CoV-2 universal vaccine, resembling the influenza hemagglutinin stem subunit, which elicits broad immune protection against different influenza viruses.[65–68]

In light of the ongoing pandemic, the rapid accumulation of mutations in S1, and the proliferation of variant strains, the immunogenicity of conserved S2 was investigated and compared to the wild-type S (Wt) and Pre in mice. We also enhanced protein immunogenicity by generating double-layered protein nanoparticles with Pre cores and S2 shells. The nonclinical safety studies of the protein nanoparticles were also carried out in this study. The results demonstrated the potential of the layered protein nanoparticles to be developed into a universal SARS-CoV-2 vaccine.

2. Result

2.1. Conservation of Spike Protein

The phylogram of seven different human coronaviruses (hCoVs) spike proteins (Table S1, Supporting Information) is shown in **Figure 1**A. The S1 and S2 phylograms (Figure 1B,C) were generated to compare their conservation (Figure 1D). Human CoVs have the same position in the S1 and S2 phylograms. However, the phylogenic distance in S2 is shorter than S1 and shows that S2 is more conserved than S1 (Figure 1E). Although S2 (588 aa, residues 686–1273) is smaller than S1 (672 aa, residues 14–685) in SARS-CoV-2, there are more conserved amino acids in S2 (Figure S1 and Table S2, Supporting Information). In addition, more mutations were found in S1 when the major SARS-CoV-2 variants were compared up to date (**Table 1**). The sequence analysis demonstrated that the S2 protein has higher conservation between subgenus and different lineages, indicating the potential of S2-based universal vaccines for SARS-CoV-2, even the entire beta-coronavirus spectrum.

2.2. Construction, Purification, and Characterization of Recombinant Proteins

SARS-CoV-2 trimeric Pre, Wt, and S2 with T4 fibritin trimerization motif, HRV3C protease cleavage site, Twin Strep Tag, and 8x His-Tag compositions are shown in **Figure 2**A. After expression and purification, Coomassie blue staining and western blot analysis confirmed the recombinant proteins by their molecular weights and binding activities to specific antibodies, respectively (Figure 2B). The investigation revealed that Wt had a metastable state due to the furin cleavage sites. Three bands appeared in purified Wt, referring to full-length S, cleaved S1, and S2 products. Meanwhile, both stable Pre and S2 showed a single band after purification. Additionally, the trimers of non-reduced recombinant protein samples were also identified by Coomassie blue staining (Figure S2A, Supporting Information).

The RBD binding activity to ACE2 was analyzed after purification. Notably, Pre and Wt were shown to have higher binding activities than S2 to hACE2/293T cells by flow cytometry (Figure 2C) and immunofluorescent assays (Figure 2E). The results were consistent with outcomes observed in the enzyme-linked immunosorbent assay (ELISA) when ACE2 protein was used as the coating antigen (Figure 2D). Therefore, purified Pre and Wt retained binding activity to ACE2. By contrast, S2 did not show ACE2-binding activity.

2.3. Humoral and Cellular Immune Response after Recombinant Protein Vaccination

To select the optimal antigen for subsequent protein nanoparticle production and vaccine studies, the immunogenicity of the recombinant proteins was investigated for antigen-specific serum antibody titers by ELISA. Mouse groups were intramuscularly immunized twice at a 4-week interval with 1 μg of Pre, Wt, and S2, respectively.

Two weeks post-boost-vaccination, comparable antibody binding titers were observed in the Pre, Wt, and S2 groups to Pre and Wt (**Figure 3**A,D). As expected, the S2 group showed higher S2-specific antibody titers than the Pre and Wt groups (Figure 3G). Notably, more IgG1 antibodies than IgG2a antibodies were elicited after the booster immunization in all groups (Figure 3B,E,H), indicating that the recombinant protein immunization generated Th2-biased antibody responses. However, S2 induced a significantly lower IgG1/IgG2a ratio than Pre and Wt (Figure 3C,F,I). Therefore, S2 induced more balanced immunoglobulin G (IgG) antibodies than Pre and Wt groups.

T-cell immune responses are an essential part of the host immune response to viral clearance. All three proteins elicited significantly high interleukin 4 (IL-4) secreting cell frequency stimulated with S or S2 protein (**Figure 4**A). In addition, a number of antigen-specific IgG antibody-secreting cells (ASCs) in the bone marrow were tested 14 days post-boost-immunization by enzyme-linked immune absorbent spot (ELISPOT) (Figure 4B). The S2 group showed significantly higher S2-specific ASC frequency than the Pre and Wt groups.

Antibody-dependent cellular cytotoxicity (ADCC) is an essential immune mechanism that limits and contains viral infections. After vaccination with recombinant proteins, S2 elicited more efficient ADCC activity than Pre or Wt (Figure 4C). Importantly, the S2 protein produced comparable serum ADCC activity to multiple variants' S proteins (Figure 4D).

Furthermore, neutralizing antibodies are critical to limiting virus replication. To study these antibodies, vesicular stomatitis virus (VSV)-based pseudoviruses expressing SARS-CoV-2 spike

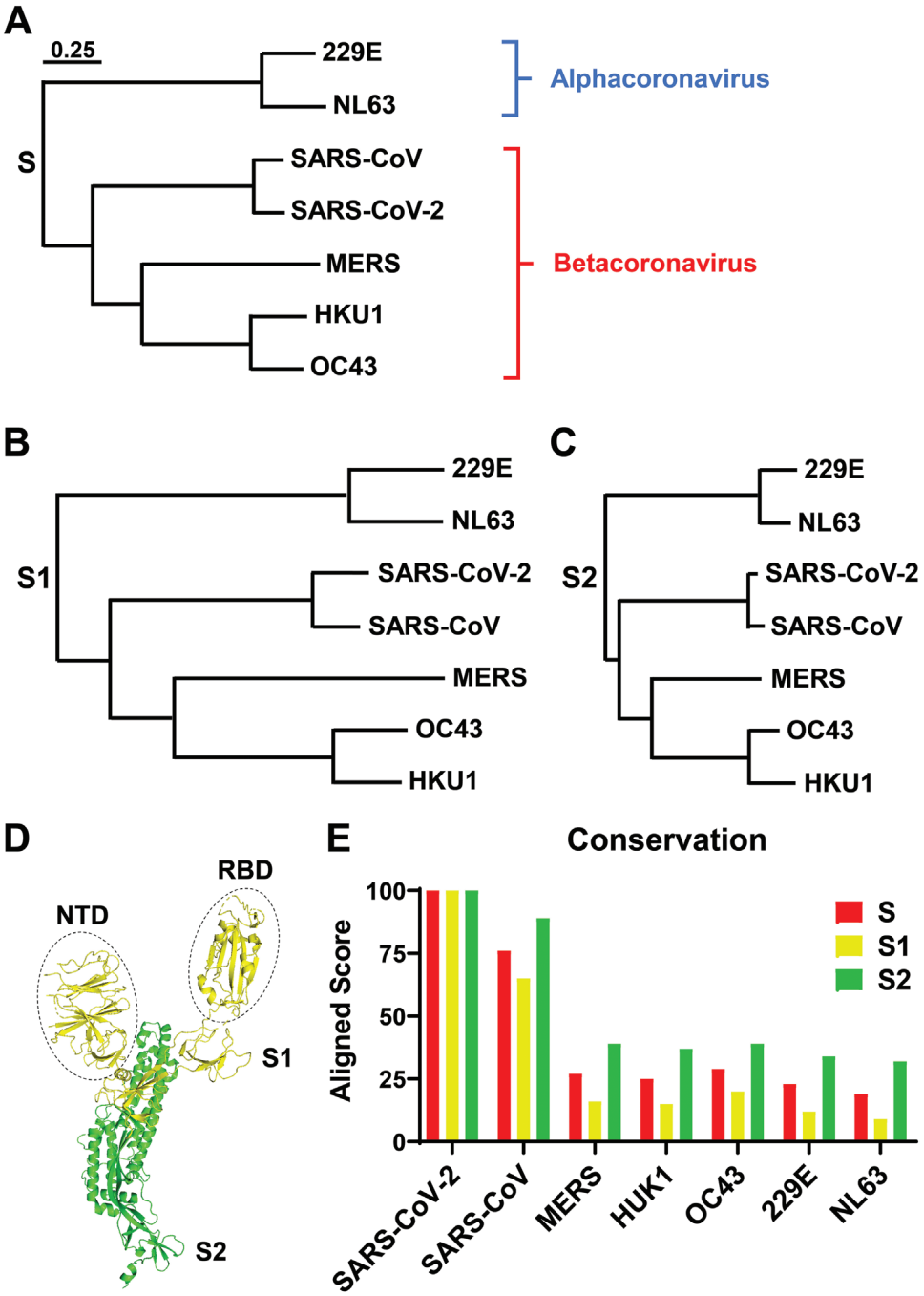

Figure 1. Phylogram and conservation of various S protein components. Phylogram of A) S, B) S1, and C) S2. The braces indicate classifications of different hCoVs. D) The structure of a single S protomer with rotated up RBD (PDB 6VSB). The S1 and S2 are shown in yellow and green, respectively. The dashed oval exhibits the N-terminal domain (NTD) and RBD. E) The S, S1, and S2 sequence conservation in comparison with SRAS-CoV-2.

proteins were used to analyze the neutralization of immune sera (Figure 4E). Ultimately, the Pre group showed the highest neutralizing antibody levels than Wt and S2 groups. Therefore, the Pre group had the most robust ability to inhibit virus entry based on the neutralization assay data, and the S2 group produced elicited significantly higher ADCC activity than other groups, demonstrating that S2 conferred protection through terminating infected cells rather than blocking cell infection.

2.4. Characterization of Nanoparticles

To improve the immunogenicity, the Pre and S2 proteins were fabricated into double-layered protein nanoparticles by ethanol desolvation and 3,3′-dithiobis[sulfosuccinimidyl propionate] (DTSSP) cross-linking (**Figure 5**A). Nanoparticle compositions of Pre/S2 (core/shell) were analyzed with sodium dodecyl sulfate–polyacrylamide gel electrophoresis

Table 1. The spike protein mutation sites of SARS-CoV-2 variants. The information comes from outbreak.info (available online: https://outbreak.info/).

		SARS-CoV-2	B.1.1.7 (α)	B.1.351 (β)	P.1 (γ)	P.2 (ζ)	P.3 (θ)	B.1.427 (ε)	B.1.525 (η)	B.1.526 (ι)	B.1.617.1 (κ)	B.1.617.2 (δ)	C.37 (λ)	B.1.621 (μ)	BA.1 (ο)
S1		L5								L5F					
		S13						S13I							
	NTD	L18			L18F										
		T19										T19R			
		T20			T20N										
		P26			P26S										
		Q52							Q52R						
		A67							A67V						A67V
		H69	del69						del69						del69
		V70	del70						del70						del70
		G75											G75V		
		T76											T76I		
		D80		D80A											
		T95								T95I				T95I	T95I
		D138			D138Y										
		G142													G142D
		V143													del143
		Y144	del144						del144					Y144S	del144
		Y145	del145						del145					Y145N	del145
		W152						W152C							
		E156										E156G			
		F157										del157			
		R158										del158			
		R190			R190S										
		N211													N211I
		L212													del212
		D215		D215G											
		R246											R246N		
		S247											del247		
		D253								D253G			del253		
		G339													G339D
		R346												R346K	
		S371													S371L
		S373													S373P
		S375													S375F
	RBD	K417		K417N	K417T										
		L452						L452R			L452R	L452R	L452Q		
		S477													S477N
		T478										T478K			T478K
		E484		E484K	E484K	E484K	E484K		E484K		E484Q			E484K	E484A
		F490											F490S		
		Q493													Q493R
		G496													G496S
		Q498													Q498R
		N501	N501Y	N501Y	N501Y		N501Y							N501Y	N501Y

Table 1. Continued.

	SARS-CoV-2	B.1.1.7 (α)	B.1.351 (β)	P.1 (γ)	P.2 (ζ)	P.3 (θ)	B.1.427 (ε)	B.1.525 (η)	B.1.526 (ι)	B.1.617.1 (κ)	B.1.617.2 (δ)	C.37 (λ)	B.1.621 (μ)	BA.1 (ο)
	Y505													Y505H
	T547													T547K
	A570	A570D												
	D614	D614G	D614G	D614G	D614G	D614G	D614G	D614G	D614G	D614G	D614G	D614G	D614G	D614G
	H655			H655Y										H655Y
	Q677							Q677H						
	N679													N679K
	P681	P681H				P681H				P681R	P681R		P681H	P681H
S2	A701		A701V											
	T716	T716I												
	D796													D796Y
	N856													N856K
	T859											T859N		
	F888							F888L						
	D950										D950N		D950N	
	Q954													Q954H
	N969													N969K
	L981													L981F
	S982	S982A												
	T1027			T1027I										
	E1092					E1092K								
	H1101					H1101Y								
	D1118	D1118H												
	V1176			V1176F	V1176F	V1176F								

(SDS-PAGE) (Figure 5B). Morphological observation by transmission electron microscopy (TEM) demonstrated the resulting nanoparticles' relatively spherical structures with irregular surfaces (Figure 5C). Pre/S2 (272.6 nm) was larger than Pre core (210.8 nm) (Figure 5D). In addition, the resulting nanoparticles showed an average zeta potential of −25 mV (Figure 5E), demonstrating their stable colloidal features.

2.5. Immune Responses Generated by Double-Layered Protein Nanoparticles

Antigen-specific serum antibody titers were determined by ELISA two weeks after the booster vaccination. As shown in **Figure 6**, nanoparticle groups (Nano) elicited higher IgG and IgG isotype antibodies than soluble protein mixtures (Solu) groups (Figure 6A,C). Notably, the ratios of IgG1/IgG2a were significantly lower in Pre- and S2-coated Nano groups (Figure 6B,D). Therefore, the higher and more balanced IgG isotype antibody titers elicited in the Nano group indicated stronger protection and less inflammation induction.

ADCC activity was analyzed with immune sera collected two weeks post-boost-immunization (Figure 6E). The Nano group generated significantly higher ADCC activity than other groups.

Immune serum neutralization activity induced by double-layered nanoparticles and soluble recombinant proteins was analyzed by neutralizing VSV-based pseudovirus infectivity (Figure S3A–D, Supporting Information). The 50% inhibitory concentration (IC_{50}) of treatment groups indicated that the Nano group elicited more effective neutralizing antibodies than other groups against SARS-CoV-2, D614G, B.1.1.7, and B.1.351 pseudovirus. Meanwhile, the Pre showed higher neutralizing antibody levels than S2 against different pseudoviruses (Figure 6F). Additionally, the Nano groups demonstrated higher IC_{50} than the corresponding Solu groups (Figure S3F, Supporting Information).

As can be seen, double-layered protein nanoparticles enhanced serum neutralizing antibody titers and triggered more balanced IgG subtypes. In addition, the Nano group generated higher ADCC activity than other groups.

We analyzed the immune responses four months (4M) after the booster immunizations to evaluate the longevity of the induced immunity. The Nano group demonstrated reduced ADCC activities after four months (Figure S3E, Supporting Information), and the 4M serum neutralization of SARS-CoV-2 pseudoviruses (Figure S3F, Supporting Information) declined compared with the 2W samples. Nonetheless, the Nano groups showed higher neutralization in 4M immune

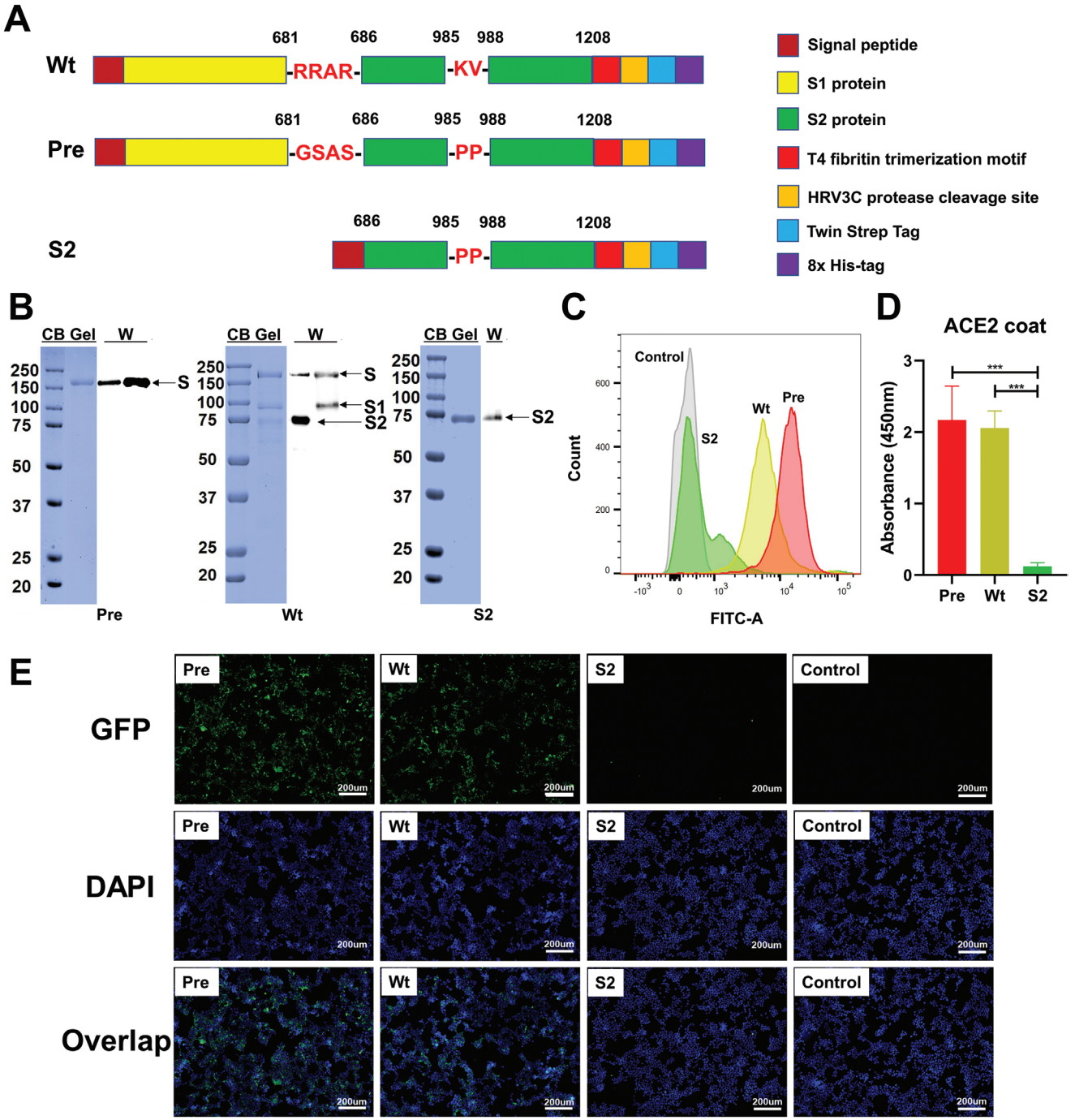

Figure 2. Recombinant protein construction, identification, and activity. A) Diagrams of Wt, Pre, and S2 compositions. The furin cleavage site RRAR (residues 682–685) was replaced with GSAS in Pre, and the residues 986 and 987 were replaced with proline substitutions both in Pre and S2. The T4 fibritin trimerization motif, HRV3C protease cleavage site, Twin Strep Tag, and 8xHis-Tag were added to the C-terminal of recombinant protein. B) Identification of purified recombinant proteins with Coomassie blue staining (CB Gel) and Western blot (W). The Pre and Wt were identified with both His-tag antibody and RBD antibody in Western blot. S2 was identified via His-tag antibody. The binding activity between recombinant proteins and ACE2 protein expressed on 293T cells' surfaces was analyzed by C) flow cytometry and E) immunofluorescence with DyLight 488. D) The binding activity of recombinant proteins and ACE2 protein ($n = 3$). Data are presented as mean ± SD. The statistical significance was analyzed with one-way ANOVA followed by Tukey's test ($^{*}p < 0.05$, $^{**}p < 0.01$, $^{***}p < 0.001$).

sera than their corresponding Solu groups in 2W (Figure S3F, Supporting Information), indicating the effectiveness of protein nanoparticles in the induction of long-lasting antibody responses.

2.6. Safety of Double-Layered Nanoparticles in Mice

Metrics for side effects were analyzed to evaluate the safety of the resulting double-layered nanoparticles. In the evaluations,

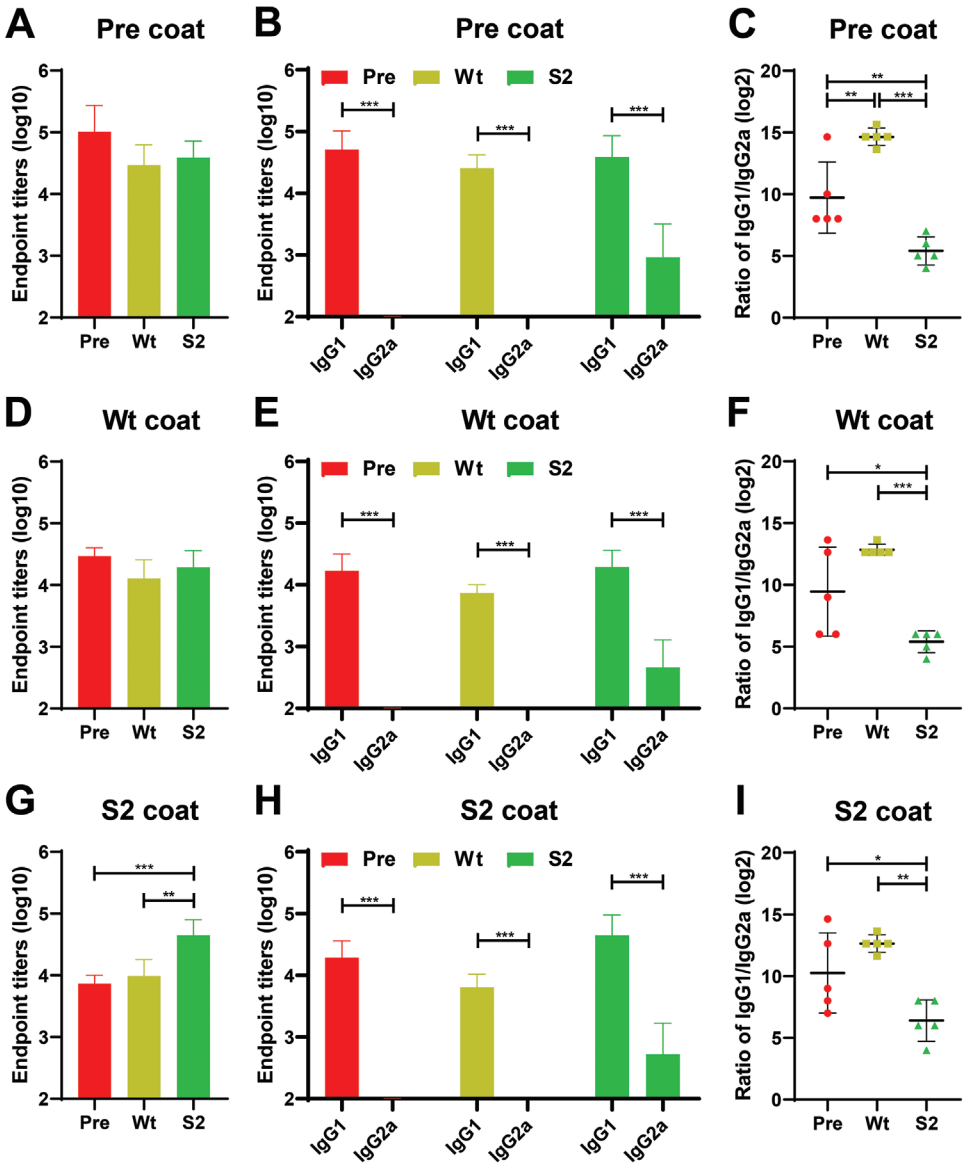

Figure 3. The specific sera antibody titers of mice immunized with recombinant proteins. Sera collected two weeks after booster vaccination were analyzed for the specific serum IgG antibody titers against A) Pre, D) Wt, and G) S2. The IgG isotype antibody titers and IgG1/IgG2a isotype ratio were measured two weeks after the last vaccination with plates coated with B,C) Pre, E,F) Wt, and H,I) S2 ($n = 5$). The data show the mean ± SD, expressed as log10 the highest dilution fold or log2 the ratio of IgG1/IgG2a, analyzed with one-way ANOVA followed by Tukey's test (*$p < 0.05$, **$p < 0.01$, ***$p < 0.001$).

no apparent detrimental physical consequences or edema were observed at the injection sites after the priming and boosting immunizations with nanoparticles (**Figure** 7A and Figure S4A (Supporting Information)). The body weight of immunized mice remained stable for three days in groups vaccinated with nanoparticles (Nano), soluble proteins (Solu), or phosphate-buffered saline (PBS) (Figure 7B and Figure S4B (Supporting Information)). Liver and kidney functions were evaluated by levels of alanine transaminase (ALT) and creatinine, respectively (Figure 7C,D and Figure S4C,D (Supporting Information)). There was no significant change in ALT and creatinine during the three-day windows after priming or boosting immunization.

Moreover, the major inflammatory cytokines IL-6 and tumor necrosis factor alpha (TNF-α) also remained level during this period (Figure 7E,F and Figure S4E,F (Supporting Information)). Finally, no inflammation was observed in the muscle tissue sections of the injection site after hematoxylin and eosin (H&E) staining in either Nano, Solu, or PBS groups (Figure 7G and Figure S4G (Supporting Information)). In this case, no apparent side effects were found after priming or boosting immunizations with double-layered protein nanoparticles.

3. Discussion

In 2002 and 2012, the lethal zoonotic beta coronavirus diseases SARS-CoV and Middle East respiratory syndrome broke out in human populations with 10% and 35% fatality rates,

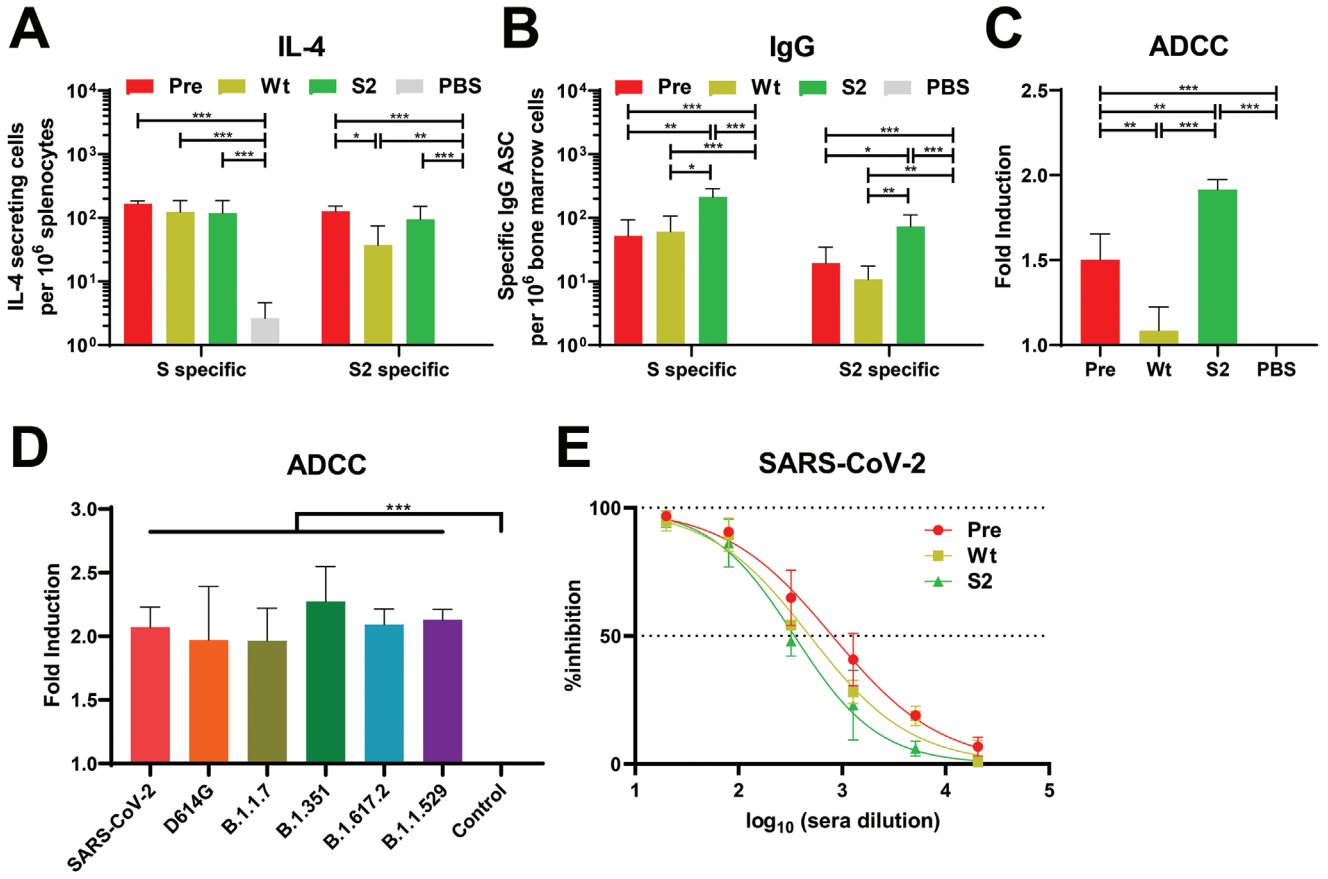

Figure 4. Cellular and humoral immune responses of vaccinated mice. A) S- and S2-specific T-cell immune responses. S- and S2-stimulated IL-4 secreting cell clones were analyzed 14 days after the booster immunization. B) Frequency of S- and S2-specific ASC per million bone marrow cells. C) ADCC activity of recombinant proteins sera at 20% serum dilution after two weeks of booster immunization, SARS-CoV-2 S protein transiently transfected HEK293T cells were used as target cells. D) S2 sera ADCC activity against multiple variants' S protein transiently transfected HEK293T cells. E) Neutralization curves of pooled sera from five mice two weeks post-boost-immunization against VSV–SARS-CoV-2. Data are presented as mean ± SD ($n = 3$). The statistical significance was analyzed with one-way ANOVA followed by Tukey's test (*$p < 0.05$, **$p < 0.01$, ***$p < 0.001$).

respectively.[69,70] More recently and more seriously, the current SARS-CoV-2 pandemic has caused millions of deaths and continues to be a significant pathogen of severe public health burden.[1,2] The prefusion S protein has been used as the major antigen in vaccines against this ongoing pandemic.[39,44–48] However, as the number of infections continues to rise, more and more variants have appeared and supplanted the ancestral virus. For this reason, the efficacy and protection of current vaccines are under constant threat and need continuous improvement.

In our work, Pre elicited the most efficient neutralization against VSV–SARS-CoV-2, D614G, B.1.1.7, and B.1.351. The S1 subunit contains the primary neutralizing antibody epitopes.[36] However, S1 is more variable than S2 (Table 1), with frequent mutating sites across different coronavirus lineages. Frequently, S1 mutations have enhanced the function of transmission or partially circumvented immunity.[4–15] Recent studies have proven that the Omicron variant has robustly escaped from the current vaccines and therapeutic monoclonal antibodies.[29–35]

By contrast, S2 is more conserved and has fewer mutations across lineages. Although S2-driven antibodies could not inhibit the binding between ACE2 and viruses, S2-specific antibodies carried out effector functions through different mechanisms with a broadly reactive spectrum. S2-specific antibody likely prevents S protein refolding from the prefusion to the postfusion state and blocks viral entry.[60] Indeed, our data confirmed that S2 stem induced effective antibody neutralization against different variants. Additionally, mouse IgG2a is known to mediate ADCC through activation of mFcγRIV. With the higher IgG2a titer, S2 elicited significantly stronger ADCC activity than other groups against multiple variants' S protein, including the most heavily mutated variant B.1.1.529. Likewise, strong cellular immune responses were also detected in the S2 groups after the booster immunizations. In effect, this work shows that the S2 stem subunit could be a potential antigen for a SARS-CoV-2 universal vaccine against unpredictable variants.

The nanoparticle platform displayed improved antigen-presenting cell uptake, enhanced cellular and humoral immune responses, and reduced antigen proteolytic degradation.[71–75] Some nanoparticle designs for covid-19 have already been validated at the clinical stage.[76–81] To improve the immunogenicity of Pre and S2, the two proteins were incorporated into double-layered protein nanoparticles. The resulting nanoparticles

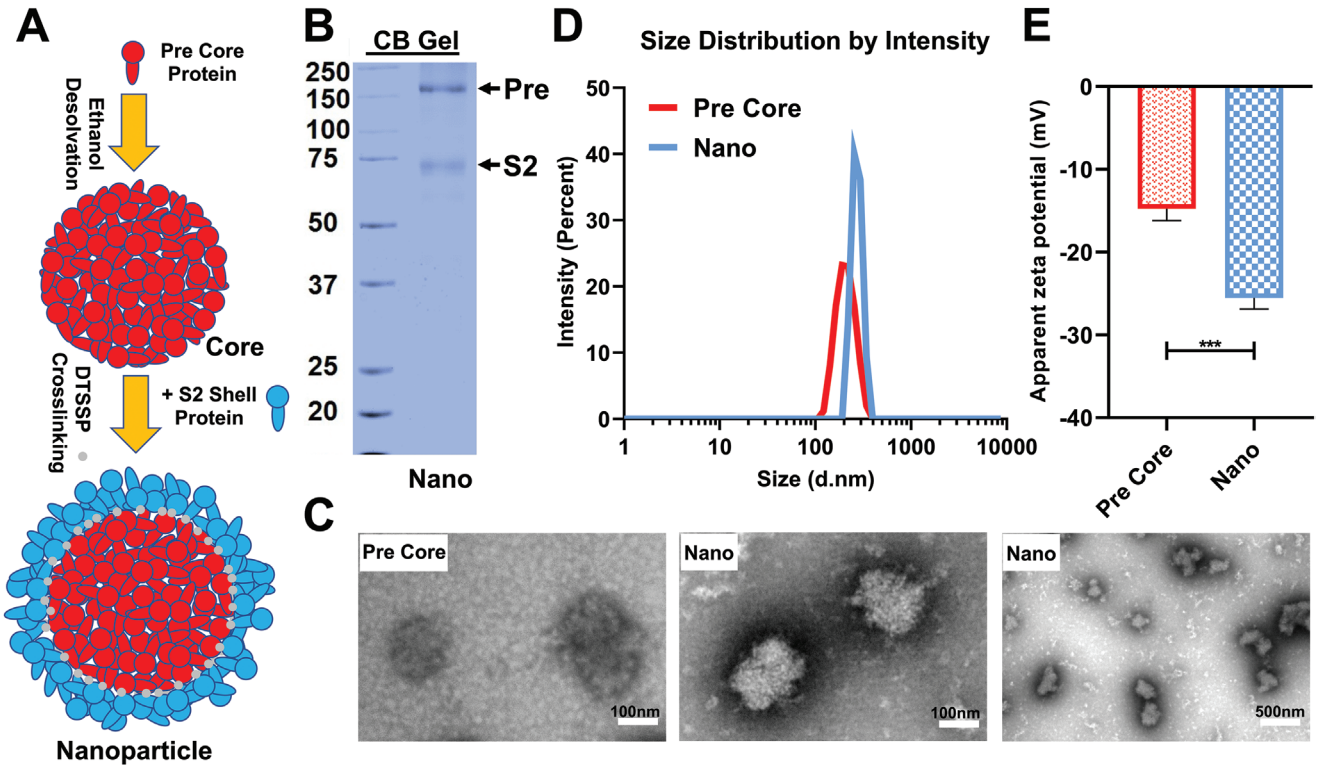

Figure 5. Fabrication and characterization of double-layered protein nanoparticles. A) The fabrication process of double-layered protein nanoparticles by cross-linking S2 shell protein on desolvated Pre core. B) Identification of double-layered nanoparticles with Coomassie blue staining (CB Gel). C) TEM image of core and nanoparticles. D) Size distribution of Pre core and Pre/S2 nanoparticles. E) Zeta potential distribution of nanoparticles (n = 3). Data are presented as mean ± SD. The statistical significance was analyzed with an unpaired t-test (***$p < 0.001$).

significantly enhanced virus-neutralizing titers and ADCC activity. Particularly, protein-nanoparticle-induced antibody neutralization lasted at least four months. In addition, more balanced antibody immune responses were detected in the nanoparticle groups, which could achieve safe and effective humoral immunity performance. Finally, the injection site adverse reaction examination, body weight, blood chemistry data, and H&E staining of muscle tissue at the injection sites did not show significant changes after the priming and boosting immunizations, suggesting that the double-layered nanoparticles have high tolerability in mice.

Overall, the conserved S2 stem subunit demonstrated its potential as a universal SARS-CoV-2 vaccine candidate against unpredictable variants. As well, our double-layered protein nanoparticles incorporating Pre and S2 induced robust and long-term immune responses and exhibited a safety profile in our primary studies, providing an option for current SARS-CoV-2 vaccine development.

4. Experimental Section

Study Design: S2 stem subunits were used as a novel immunogen to induce broad protection because of the genetic conservation between subgenuses and different lineages. Double-layered protein nanoparticles were fabricated to enhance both S2 and Pre immunogenicity in mice. Animal experiments were performed to validate the vaccine designs. Experimental replicates were performed as described in each figure legend.

Ethics Statement: The "Guide for the Care and Use of Laboratory Animals" by the National Institutes of Health was faithfully adhered to in this study. All mice experiments were approved by Georgia State University Institutional Animal Care and Use Committee (IACUC) with protocol number A19025.

Construction and Activity of Recombinant Proteins Pre, Wt, and S2: The gene of wild-type spike protein (GenBank: QHR63290.2) was codon-optimized and synthesized for expression. The furin cleavage site Arg-Arg-Ala-Arg (RRAR residues 681–685) in Wt was replaced with Gly-Ser-Ala-Ser (GSAS) in Pre, and the residues 986 and 987 were replaced with proline substitutions both in Pre and S2. Compared with Pre, the S1 sequence was deleted in the S2 protein. The T4 fibritin trimerization motif, Human rhinovirus 3C (HRV3C) protease cleavage site, Twin Strep Tag, and 8xHis-Tag were added to the C-terminal of the recombinant protein.[48] The recombinant proteins' constructions are shown in Figure 2A. After being expressed with Bac-to-Bac Baculovirus Expression System (Invitrogen, Carlsbad, CA, USA) in *Spodoptera frugiperda* (Sf9) insect cells (ATCC, CRL-1711), the recombinant proteins were purified with HisPur Ni-NTA Resin (Thermo Scientific, Rockford, IL, USA).[82] Purified proteins were characterized by SDS-PAGE and Western blots probed with anti-His antibody (Cat: ab18184, Abcam) or anti-RBD antibody (Cat: 40592-T62, Sino Biological).

The binding activity of recombinant proteins to human ACE2 protein (expressed stably on the surface of 293T cells, hACE2/293T) was analyzed with anti-His antibody and DyLight 488 (Cat: 405310, Biolegend) by flow cytometry and immunofluorescence. Furthermore, the ACE2 protein (Cat: ab273687, Abcam) was also used to identify recombinant proteins' binding activity. Briefly, ACE2 protein was coated in 96-well ELISA plates (Corning Inc., NY, USA) overnight at 4 °C. After blocking with 1% bovine serum albumin (BSA), recombinant proteins were added to the plate for 2 h at 37 °C. After washing, anti-His primary antibody and horseradish peroxidase (HRP) conjugated anti-mouse secondary antibodies were

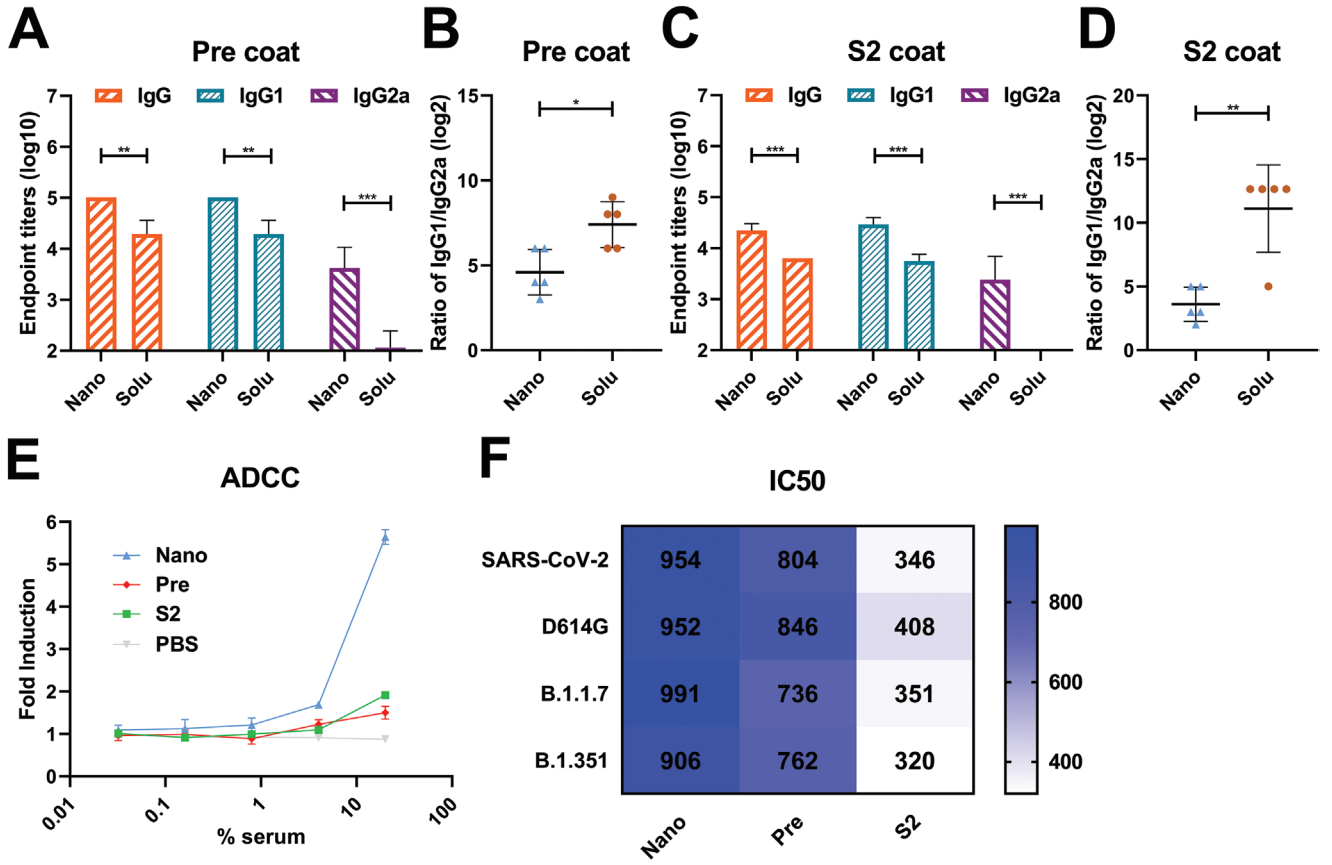

Figure 6. The humoral immune responses of mice immunized with nanoparticles. The IgG, IgG isotype antibody titers, and IgG1/IgG2a ratio were measured two weeks after the booster vaccination with plates coated with A,B) Pre, and C,D) S2 ($n = 5$). E) ADCC surrogate assay results. F) The sera IC_{50} of nanoparticles, Pre, and S2 against VSV-based pseudoviruses. Data showed mean ± SD, expressed as log10 the highest dilution fold or log2 the ratio of IgG1/IgG2a, analyzed with two-way ANOVA followed by Tukey's test (A and C) and unpaired *t*-test (B and D) (*$p < 0.05$, **$p < 0.01$, ***$p < 0.001$).

added in turn. Finally, HRP substrate 3,3′,5,5′-tetramethylbenzidine (TMB) solution (Cat: 34029, Thermo Scientific, US) was added to measure the absorbance at 450 nm.

Fabrication and Characterization of Nanoparticles: The fabrication of double-layered protein nanoparticles was similar to our previously described methods with modification.[83] The nanoparticle core was made with Pre protein undergoing desolvation of ethanol. After centrifuging at 15 000 × *g* for 20 min, the Pre core was collected and resuspended in shell protein solutions (100 µL, 0.5 µg µL^{-1} in Dulbecco's phosphate-buffered saline (DPBS) of Pre, Wt, or S2) by sonication. Thereupon, 5 × 10^{-3} M of DTSSP (Thermo Scientific, Waltham, MA) was used as a cross-linker to stabilize the core and shell proteins. After quenching the cross-linking reaction with 30 × 10^{-3} M Tris-HCl solution at pH 7.4 for 15 min, the constructed double-layered protein nanoparticles were collected by centrifugation at 15 000 × *g* at 4 °C for 30 min and resuspended by sonication in 50 µL DPBS.

Then SDS-PAGE was used to analyze the composition of the double-layered nanoparticles. Additionally, the size and zeta potential of nanoparticles were measured by dynamic light scattering analysis with Malvern Zetasizer Nano ZS (Malvern Instruments, Westborough, MA). Finally, a Jeol JEM-100CX II and Apogee Imaging Systems couple-charged device (CCD) camera system were used to take TEM images of the nanoparticles.

Immunization of Mice: Female BALB/c mice at 6–8 weeks of age were randomly distributed into groups ($n = 5$) and immunized intramuscularly (i.m.) at day 0 and boosted on day 28 with 1 µg soluble recombinant proteins (Pre, Wt, or S2) in cohort 1 (Blue) (Figure S2B, Supporting Information). In cohort 2 (green), 1 µg of double-layered protein nanoparticles (Pre/S2) or soluble protein mixtures (Pre+S2) were given i.m. at days 0 and 28. On day 42, cohort 1 and 2 samples were collected, and the T-cell responses, bone marrow responses, serum antibody titers, ADCC, and neutralization titers were analyzed. Meanwhile, after two immunizations with 1 µg nanoparticles on days 0 and 28, cohort 3 (yellow) was used to evaluate long-lasting immune responses four months post-boost-immunization.

Humoral and Cellular Immune Response Assays: The specific humoral immune responses to Pre, Wt, and S2 were assessed by ELISA.[84] Briefly, the proteins were used to coat the ELISA plates (Corning Inc., NY, USA) overnight at 4 °C. Next, after blocking with 1% BSA, fourfold serial dilutions of murine sera were added to the plate for 1 h at 37 °C. And then, after washing with phosphate-buffered saline with 0.1% Tween 20 (PBST), HRP-conjugated anti-IgG, -IgG1, or -IgG2a isotype antibodies were added for 1 h at 37 °C. Finally, a TMB solution was used to detect the absorbance at 450 nm.

Additionally, two weeks post-boost-immunization, the ADCC was tested according to the kit protocol (Cat: 1215, Promega) with modification. Briefly, the plasmid encoding the S proteins was transfected to human embryonic kidney 293T (HEK-293T) cells by Lipofectamine 3000 Transfection Reagent (Cat: L3000-015, Invitrogen). Then, two days after the transfection, serially diluted sera and mFcγRIV effector cells were added and incubated for 6 h at 37 °C. Finally, Bio-Glo Luciferase assay substrate (Promega) was added at ambient temperature (22–25 °C) for 5 min. The luminescence relative light unit (RLU) was read by GloMax (Promega), and fold induction was calculated with the following formula: fold induction = RLU (induced – background)/RLU (no antibody control – background).

As previously described, VSVs containing SARS-CoV-2 spike envelope glycoproteins were established.[85] Briefly, 293T cells were transfected with

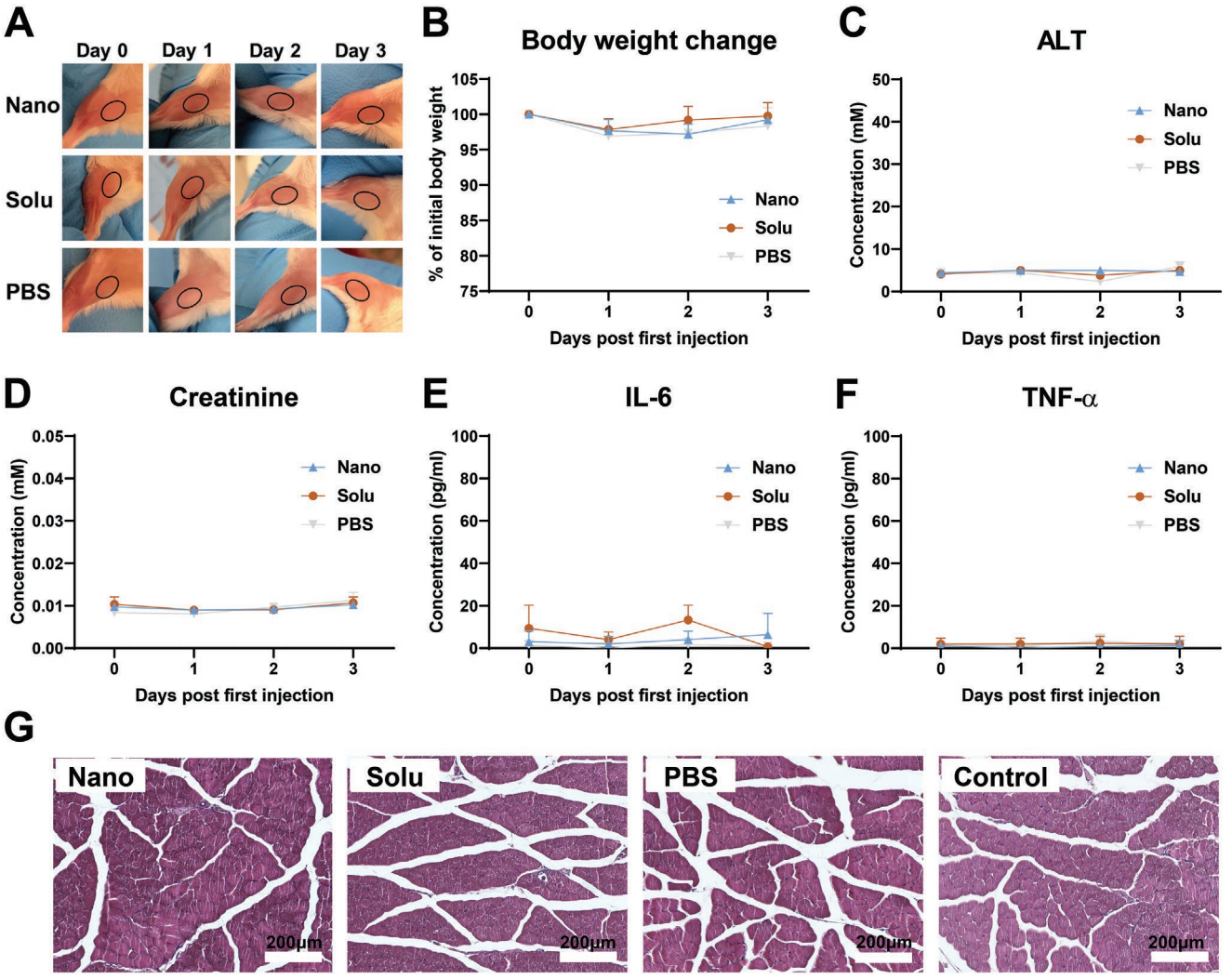

Figure 7. Nanoparticle safety in mice. A) Injection site adverse reaction examination and B) body weight change three days post-prime-immunization. C–F) Concentration changes of ALT (C), creatinine (D), IL-6 (E), and TNF-α (F) in sera before and after prime immunization. G) H&E staining of muscle tissue at the injection site. Data are presented as mean ± SD ($n = 3$). Statistical significance was analyzed with one-way ANOVA followed by Tukey's test.

plasmid encoding SARS-CoV-2, D614G (Cat: 158075, Addgene), B.1.1.7 (Cat: VG40771-UT, Sino Biological), or B.1.351 (Cat: VG40772-UT, Sino Biological) spike protein gene. Next, after one day of incubation at 37 °C with 5% CO_2, 3 MOI of pseudotyped ΔG-luciferase (G*ΔG-luciferase) recombinant vesicular stomatitis virus (rVSV) (Cat: EH1025-PM, Kerafast) was added to infect the cell for 2 h. Eventually, after washing and culturing for 30 h until cytopathic effect (CPE) showed in most cells, the supernatant was collected by centrifugation at 500*g* for 10 min and stored at −80 °C. The pseudovirus neutralization assay was performed by incubating recombinant VSV with serial dilutions of mice sera for 1 h at 37 °C. Then, the mixture of rVSV and mice sera was added into hACE2/293T for 24 h of incubation. After the incubation, the luminescence was read by GloMax (Promega), and the IC_{50} was calculated with GraphPad Prism 8.0.

IL-4 ELISPOT assays were performed as previously described.[83] Briefly, ELISPOT plates (BD Biosciences) were coated overnight at 4 °C with murine IL-4 specific monoclonal antibodies. Once the plates were prepared, splenocytes collected 14 days after the booster immunization were added to the wells and stimulated with S protein (Cat: 40589-V08B1, Sino Biological) or S2 protein (Cat: 40590-V08B, Sino Biological). After incubation at 37 °C for 48 h, biotinylated IL-4 antibodies were added to the plates for 2 h and peroxidase-labeled streptavidin for another 1 h. After washing, the peroxidase substrate was added, and spots were monitored with Bioreader-6000-E (Biosys, Germany).

ELISPOT plates (BD Biosciences) coated with S protein (Sino Biological) or S2 protein (Sino Biological) were used to detect the bone marrow plasma cells after 14 days of booster immunization. After washing and blocking, bone marrow cells were added to plates and incubated at 37 °C for 18 h. Once the incubation was complete, the spots were visualized by HRP-conjugated goat anti-mouse IgG antibody and peroxidase substrate. A Bioreader-6000-E (Biosys) was used to read and analyze the data.

Safety of Nanoparticles in Mice: The safety of the double-layered nanoparticles in mice was analyzed after prime and boost i.m. immunizations with 1 μg of nanoparticles (Nano) in the BALB/c mice ($n = 3$). Soluble protein solutions (Solu) and PBS were given as controls. The physical injury or edema of the injection site and body weight change were recorded daily for three days after injection. Sera samples were collected before and 1, 2, and 3 days after injection. Additionally, liver and kidney functions were determined postimmunization with ALT activity assay kits (Cat: ab105134, Abcam) and creatinine assay kits (Cat: ab65340, Abcam). Furthermore, the inflammatory cytokines IL-6 and TNF-α in sera were analyzed with Mouse IL-6 Uncoated ELISA kit (Cat: 88-7064-88, Invitrogen) and Mouse TNF-α Uncoated ELISA kit (Cat: 88-7324-88, Invitrogen) to evaluate inflammation after double-layered nanoparticles vaccination. Moreover, injection site muscle tissue was harvested and fixed in 10% formalin. After paraffin embedding and cutting, the 10 μm thick tissue sections were stained with H&E and observed for inflammation.

Statistical Analysis: Statistical analyses were performed with GraphPad Prism 8. The data were presented as means with standard derivation (SD). Correlations were calculated with one-way or two-way analysis of variance (ANOVA) followed by the Tukey's test or an unpaired *t*-test. Only data resulting in p values < 0.05 were regarded as statistically significant for all tests.

Supporting Information

Supporting Information is available from the Wiley Online Library or from the author.

Acknowledgements

The authors thank David D. Ho lab in the Columbia University Vagelos College of Physicians and Surgeons for providing hACE2/293T cells. Funding: this work was supported by the US National Institutes of Health (NIH)/National Institute of Allergy and Infectious Diseases (NIAID) under Grant Nos. AI101047, AI116835, and AI143844 to B.-Z.W. The electron microscopy study was performed at the Georgia Institute of Technology for Electronics and Nanotechnology, a member of the National Nanotechnology Coordinated Infrastructure (NNCI). Table of contents figure was created with BioRender.com. The content in this study was solely the authors' responsibility and did not necessarily represent the official views of the funders.

Conflict of Interest

The authors declare no conflict of interest.

Author Contributions

Conceptualization: Y.M., B.-Z.W., methodology: Y.M., formal analysis: Y.M., investigation: Y.M., Y.W., C.D., G.X.G., W.Z., J.K., L.W., resources: S.-M.K., B.-Z.W., writing-original draft: Y.M., writing-review and editing: Y.M., C.D., G.X.G., J.K., S.-M.K., B.Z.-W., supervision: B.-Z.W., project administration: B.-Z.W., funding acquisition: B.-Z.W.

Data Availability Statement

The data that support the findings of this study are available from the corresponding author upon reasonable request.

Keywords

antibody-dependent cellular cytotoxicity, conserved S2 stem subunit, double-layered protein nanoparticles, prefusion spike protein, SARS-Cov-2 variants

Received: February 8, 2022
Revised: April 1, 2022
Published online: May 23, 2022

[1] WHO Coronavirus Disease (COVID-19) Dashboard, https://covid19.who.int/ (accessed: February 2022).
[2] Na Zhu, D. Zhang, W. Wang, X. Li, Bo Yang, J. Song, X. Zhao, B. Huang, W. Shi, R. Lu, P. Niu, F. Zhan, X. Ma, D. Wang, W. Xu, G. Wu, G F. Gao, W. Tan, *N. Engl. J. Med.* **2020**, *382*, 727.
[3] P. Zhou, X.-L. Yang, X.-G. Wang, B. Hu, L. Zhang, W. Zhang, H.-R. Si, Y. Zhu, B. Li, C.-L. Huang, H.-D. Chen, J. Chen, Y. Luo, H. Guo, R.-D. Jiang, M.-Q. Liu, Y. Chen, X.-R. Shen, X. Wang, X.-S. Zheng, K. Zhao, Q.-J. Chen, F. Deng, L.-L. Liu, B. Yan, F.-X. Zhan, Y.-Y. Wang, G.-F. Xiao, Z.-L. Shi, *Nature* **2020**, *579*, 270.
[4] N. G. Davies, S. Abbott, R. C. Barnard, C. I. Jarvis, A. J. Kucharski, J. D. Munday, C. A. B. Pearson, T. W. Russell, D. C. Tully, A. D. Washburne, T. Wenseleers, A. Gimma, W. Waites, K. L. M. Wong, K. van Zandvoort, J. D. Silverman, K. Diaz-Ordaz, R. Keogh, R. M. Eggo, S. Funk, Mark Jit, K. E. Atkins, W. J. Edmunds, *Science* **2021**, *372*.
[5] N. G. Davies, C. I. Jarvis, W. J. Edmunds, N. P. Jewell, K. Diaz-Ordaz, R. H. Keogh, *Nature* **2021**, *593*, 270.
[6] P. Wang, M. S. Nair, L. Liu, S. Iketani, Y. Luo, Y. Guo, M. Wang, J. Yu, B. Zhang, P. D. Kwong, B. S. Graham, J. R. Mascola, J. Y. Chang, M. T. Yin, M. Sobieszczyk, C. A. Kyratsous, L. Shapiro, Z. Sheng, Y. Huang, D. D. Ho, *Nature* **2021**, *593*, 130.
[7] K. Wu, A. P. Werner, M. Koch, A. Choi, E. Narayanan, G. B. E. Stewart-Jones, T. Colpitts, H. Bennett, S. Boyoglu-Barnum, W. Shi, J. I. Moliva, N. J. Sullivan, B. S. Graham, A. Carfi, K. S. Corbett, R. A. Seder, D. K. Edwards, *N. Engl. J. Med.* **2021**, *384*, 1468.
[8] Y. Liu, J. Liu, H. Xia, X. Zhang, C. R. Fontes-Garfias, K. A. Swanson, H. Cai, R. Sarkar, W. Chen, M. Cutler, D. Cooper, S. C. Weaver, A. Muik, U. Sahin, K. U. Jansen, X. Xie, P. R. Dormitzer, P.-Y. Shi, *N. Engl. J. Med.* **2021**, *384*, 1466.
[9] C. K. Wibmer, F. Ayres, T. Hermanus, M. Madzivhandila, P. Kgagudi, B. Oosthuysen, B. E. Lambson, T. de Oliveira, M. Vermeulen, K. van der Berg, T. Rossouw, M. Boswell, V. Ueckermann, S. Meiring, A. von Gottberg, C. Cohen, L. Morris, J. N. Bhiman, P. L. Moore, *Nat. Med.* **2021**, *27*, 622.
[10] H. Tegally, E. Wilkinson, M. Giovanetti, A. Iranzadeh, V. Fonseca, J. Giandhari, D. Doolabh, S. Pillay, E. J. San, N. Msomi, K. Mlisana, A. von Gottberg, S. Walaza, M. Allam, A. Ismail, T. Mohale, A. J. Glass, S. Engelbrecht, G. Van Zyl, W. Preiser, F. Petruccione, A. Sigal, D. Hardie, G. Marais, N.-Y. Hsiao, S. Korsman, M.-A. Davies, L. Tyers, I. Mudau, D. York, et al., *Nature* **2021**, *592*, 438.
[11] A. Chandrashekar, J. Liu, J. Yu, K. Mcmahan, L. H. Tostanoski, C. Jacob-Dolan, N. B. Mercado, T. Anioke, A. Chang, S. Gardner, V. M. Giffin, D. L. Hope, F. Nampanya, S. Patel, O. Sanborn, D. Sellers, H. Wan, A. J. Martinot, J. J. Baczenas, S. L. O'connor, L. Pessaint, D. Valentin, B. Espina, L. Wattay, M. G. Ferrari, R. Brown, A. Cook, D. Bueno-Wilkerson, E. Teow, H. Andersen, et al., *Sci. Transl. Med.* **2021**, *13*, eabj2641.
[12] X. Shen, H. Tang, R. Pajon, G. Smith, G. M. Glenn, W. Shi, B. Korber, D. C. Montefiori, *N. Engl. J. Med.* **2021**, *384*, 2352.
[13] M. Hoffmann, P. Arora, R. Groß, A. Seidel, B. F. Hörnich, A. S. Hahn, N. Krüger, L. Graichen, H. Hofmann-Winkler, A. Kempf, M. S. Winkler, S. Schulz, H.-M. Jäck, B. Jahrsdörfer, H. Schrezenmeier, M. Müller, A. Kleger, J. Münch, S. Pöhlmann, *Cell* **2021**, *184*, 2384.
[14] V. V. Edara, C. Norwood, K. Floyd, L. Lai, M. E. Davis-Gardner, W. H. Hudson, G. Mantus, L. E. Nyhoff, M. W. Adelman, R. Fineman, S. Patel, R. Byram, D. N. Gomes, G. Michael, H. Abdullahi, N. Beydoun, B. Panganiban, N. Mcnair, K. Hellmeister, J. Pitts, J. Winters, J. Kleinhenz, J. Usher, J. B. O'keefe, A. Piantadosi, J. J. Waggoner, A. Babiker, D. S. Stephens, E. J. Anderson, S. Edupuganti, et al., *Cell Host Microbe* **2021**, *29*, 516.
[15] E. C. Sabino, L. F. Buss, M. P. S. Carvalho, C. A. Prete, M. A. E. Crispim, N. A. Fraiji, R. H. M. Pereira, K. V. Parag, P. da Silva Peixoto, M. U. G. Kraemer, M. K. Oikawa, T. Salomon, Z. M. Cucunuba, M. C. Castro, A. A. de Souza Santos, V. H. Nascimento, H. S. Pereira, N. M. Ferguson, O. G. Pybus,

A. Kucharski, M. P. Busch, C. Dye, N. R. Faria, *Lancet* **2021**, *397*, 452.
[16] L. M. Hagan, D. W. Mccormick, C. Lee, S. Sleweon, L. Nicolae, T. Dixon, R. Banta, I. Ogle, C. Young, C. Dusseau, S. Salmonson, C. Ogden, E. Godwin, T. Ballom, T. Ross, H. Browne, J. L. Harcourt, A. Tamin, N. J. Thornburg, H. L. Kirking, P. P. Salvatore, J. E. Tate, *Morb. Mortal. Wkly. Rep.* **2021**, *70*, 1349.
[17] M. Melloul, T. Chouati, M. Hemlali, S. Alaoui Amine, N. Touil, H. Elannaz, K. Ennibi, M. Youbi, M. Merabet, A. M. Bellefquih, J. Nourlil, A. Maaroufi, E. El Fahime, *Microbiol. Resour. Announce.* **2021**, *10*.
[18] K. Tao, P. L. Tzou, J. Nouhin, R. K. Gupta, T. de Oliveira, S. L. Kosakovsky Pond, D. Fera, R. W. Shafer, *Nat. Rev. Genet.* **2021**, *22*, 757.
[19] A. Sheikh, J. Mcmenamin, B. Taylor, C. Robertson, *Lancet* **2021**, *397*, 2461.
[20] F. Campbell, B. Archer, H. Laurenson-Schafer, Y. Jinnai, F. Konings, N. Batra, B. Pavlin, K. Vandemaele, M. D Van Kerkhove, T. Jombart, O. Morgan, O. l. P. de Waroux, *Eurosurveillance* **2021**, *26*.
[21] E. C. Wall, M. Wu, R. Harvey, G. Kelly, S. Warchal, C. Sawyer, R. Daniels, P. Hobson, E. Hatipoglu, Y. Ngai, S. Hussain, J. Nicod, R. Goldstone, K. Ambrose, S. Hindmarsh, R. Beale, A. Riddell, S. Gamblin, M. Howell, G. Kassiotis, V. Libri, B. Williams, C. Swanton, S. Gandhi, D. L. Bauer, *Lancet* **2021**, *397*, 2331.
[22] T. Farinholt, H. Doddapaneni, X. Qin, V. Menon, Q. Meng, G. Metcalf, H. Chao, M.-C. Gingras, V. Avadhanula, P. Farinholt, C. Agrawal, D. M. Muzny, P. A. Piedra, R. A. Gibbs, J. Petrosino, *BMC Medicine* **2021**, *19*.
[23] J. Lopez Bernal, N. Andrews, C. Gower, E. Gallagher, R. Simmons, S. Thelwall, J. Stowe, E. Tessier, N. Groves, G. Dabrera, R. Myers, C. N. J. Campbell, G. Amirthalingam, M. Edmunds, M. Zambon, K. E. Brown, S. Hopkins, M. Chand, M. Ramsay, *N. Engl. J. Med.* **2021**, *385*, 585.
[24] D. Planas, D. Veyer, A. Baidaliuk, I. Staropoli, F. Guivel-Benhassine, M. M. Rajah, C. Planchais, F. Porrot, N. Robillard, J. Puech, M. Prot, F. Gallais, P. Gantner, A. Velay, J. Le Guen, N. Kassis-Chikhani, D. Edriss, L. Belec, A. Seve, L. Courtellemont, H. Péré, L. Hocqueloux, S. Fafi-Kremer, T. Prazuck, H. Mouquet, T. Bruel, E. Simon-Lorière, F. A. Rey, O. Schwartz, *Nature* **2021**, *596*, 276.
[25] M. Hoffmann, H. Hofmann-Winkler, N. Krüger, A. Kempf, I. Nehlmeier, L. Graichen, P. Arora, A. Sidarovich, A.-S. Moldenhauer, M. S. Winkler, S. Schulz, H.-M. Jäck, M. V. Stankov, G. M. N. Behrens, S. Pöhlmann, *Cell Rep.* **2021**, *36*, 109415.
[26] P. Mlcochova, S. A. Kemp, M. S. Dhar, G. Papa, B. Meng, I. A. T. M. Ferreira, R. Datir, D. A. Collier, A. Albecka, S. Singh, R. Pandey, J. Brown, J. Zhou, N. Goonawardane, S. Mishra, C. Whittaker, T. Mellan, R. Marwal, M. Datta, S. Sengupta, K. Ponnusamy, V. S. Radhakrishnan, A. Abdullahi, O. Charles, P. Chattopadhyay, P. Devi, D. Caputo, T. Peacock, C. Wattal, N. Goel, et al., *Nature* **2021**, *599*, 114.
[27] E. Callaway, *Nature* **2021**, *600*, 21.
[28] R. Viana, S. Moyo, D. G. Amoako, H. Tegally, C. Scheepers, C. L. Althaus, U. J. Anyaneji, P. A. Bester, M. F. Boni, M. Chand, W. T. Choga, R. Colquhoun, M. Davids, K. Deforche, D. Doolabh, L. Du Plessis, S. Engelbrecht, J. Everatt, J. Giandhari, M. Giovanetti, D. Hardie, V. Hill, N.-Y. Hsiao, A. Iranzadeh, A. Ismail, C. Joseph, R. Joseph, L. Koopile, S. L. Kosakovsky Pond, M. U. G. Kraemer, et al., *Nature* **2022**, *603*, 679.
[29] L. Liu, S. Iketani, Y. Guo, J. F.-W. Chan, M. Wang, L. Liu, Y. Luo, H. Chu, Y. Huang, M. S. Nair, J. Yu, K. K.-H. Chik, T. T.-T. Yuen, C. Yoon, K. K.-W. To, H. Chen, M. T. Yin, M. E. Sobieszczyk, Y. Huang, H. H. Wang, Z. Sheng, K.-Y. Yuen, D. D. Ho, *Nature* **2022**, *602*, 676.
[30] Q. Wang, Y. Li, Y. Li, N. Osherov, G. H. Goldman, P. E. Verweij, B. Zheng, R. Li, W. Chen, T. Liang, Z. Wan, W. Liu, *Emerging Microbes Infect.* **2022**, *11*, 1.
[31] L. Lu, B. W.-Y. Mok, L.-L. Chen, J. M.-C. Chan, O. T.-Y. Tsang, B. H.-S. Lam, V. W.-M. Chuang, A. W.-H. Chu, W.-M. Chan, J. D. Ip, B. P.-C. Chan, R. Zhang, C. C.-Y. Yip, V. C.-C. Cheng, K.-H. Chan, D.-Y. Jin, I. F.-N. Hung, K.-Y. Yuen, H. Chen, K. K.-W. To, *Clin. Infect. Dis.* **2021**.
[32] J. Ai, H. Zhang, Y. Zhang, K. Lin, Y. Zhang, J. Wu, Y. Wan, Y. Huang, J. Song, Z. Fu, H. Wang, J. Guo, N. Jiang, M. Fan, Y. Zhou, Y. Zhao, Q. Zhang, Q. Liu, J. Lv, P. Li, C. Qiu, W. Zhang, *Emerging Microbes Infect.* **2022**, *11*, 337.
[33] L. Espenhain, T. Funk, M. Overvad, S. M. Edslev, J. Fonager, A. C. Ingham, M. Rasmussen, S. L. Madsen, C. H. Espersen, R. N. Sieber, M. Stegger, V. Gunalan, B. Wilkowski, N. B. Larsen, R. Legarth, A. S. Cohen, F. Nielsen, J. U. H. Lam, K. E. Lavik, M. Karakis, K. Spiess, E. Marving, C. Nielsen, C. Wiid Svarrer, J. Bybjerg-Grauholm, S. S. Olsen, A. Jensen, T. G. Krause, L. Müller, *Eurosurveillance* **2021**, *26*.
[34] L. T. Brandal, E. MacDonald, L. Veneti, T. Ravlo, H. Lange, U. Naseer, S. Feruglio, K. Bragstad, O. Hungnes, L. E. Ødeskaug, F. Hagen, K. E. Hanch-Hansen, A. Lind, S. V. Watle, A. M. Taxt, M. Johansen, L. Vold, P. Aavitsland, K. Nygård, E. H. Madslien, *Eurosurveillance* **2021**, *26*.
[35] C. C.-R. Team, *Morb. Mortal. Wkly. Rep.* **2021**, *70*, 1731.
[36] H. Yang, Z. Rao, *Nat. Rev. Microbiol.* **2021**, *19*, 685.
[37] B. J. Bosch, R. van der Zee, C. A. M. de Haan, P. J. M. Rottier, *J. Virol.* **2003**, *77*, 8801.
[38] B. Coutard, C. Valle, X. de Lamballerie, B. Canard, N. G. Seidah, E. Decroly, *Antiviral Res.* **2020**, *176*, 104742.
[39] A. C. Walls, Y.-J. Park, M. A. Tortorici, A. Wall, A. T. Mcguire, D. Veesler, *Cell* **2020**, *181*, 281.
[40] F. Li, *Annu. Rev. Virol.* **2016**, *3*, 237.
[41] J. Lan, J. Ge, J. Yu, S. Shan, H. Zhou, S. Fan, Q. Zhang, X. Shi, Q. Wang, L. Zhang, X. Wang, *Nature* **2020**, *581*, 215.
[42] R. Yan, Y. Zhang, Y. Li, L. Xia, Y. Guo, Q. Zhou, *Science* **2020**, *367*, 1444.
[43] A. C. Walls, M. A. Tortorici, J. Snijder, X. Xiong, B.-J. Bosch, F. A. Rey, D. Veesler, *Proc. Natl. Acad. Sci. USA* **2017**, *114*, 11157.
[44] F. P. Polack, S. J. Thomas, N. Kitchin, J. Absalon, A. Gurtman, S. Lockhart, J. L. Perez, G. Pérez Marc, E. D. Moreira, C. Zerbini, R. Bailey, K. A. Swanson, S. Roychoudhury, K. Koury, P. Li, W. V. Kalina, D. Cooper, R. W. Frenck, L. L. Hammitt, Ö. Türeci, H. Nell, A. Schaefer, S. Ünal, D. B. Tresnan, S. Mather, P. R. Dormitzer, U. Şahin, K. U. Jansen, W. C. Gruber, *N. Engl. J. Med.* **2020**, *383*, 2603.
[45] L. R. Baden, H. M. El Sahly, B. Essink, K. Kotloff, S. Frey, R. Novak, D. Diemert, S. A. Spector, N. Rouphael, C. B. Creech, J. Mcgettigan, S. Khetan, N. Segall, J. Solis, A. Brosz, C. Fierro, H. Schwartz, K. Neuzil, L. Corey, P. Gilbert, H. Janes, D. Follmann, M. Marovich, J. Mascola, L. Polakowski, J. Ledgerwood, B. S. Graham, H. Bennett, R. Pajon, C. Knightly, et al., *N. Engl. J. Med.* **2021**, *384*, 403.
[46] M. Voysey, S. A. Costa Clemens, S. A. Madhi, L. Y. Weckx, P. M. Folegatti, P. K. Aley, B. Angus, V. L. Baillie, S. L. Barnabas, Q. E. Bhorat, S. Bibi, C. Briner, P. Cicconi, E. A. Clutterbuck, A. M. Collins, C. L. Cutland, T. C. Darton, K. Dheda, C. Dold, C. J. A. Duncan, K. R. W. Emary, K. J. Ewer, A. Flaxman, L. Fairlie, S. N. Faust, S. Feng, D. M. Ferreira, A. Finn, E. Galiza, A. L. Goodman, et al., *Lancet* **2021**, *397*, 881.
[47] J. Sadoff, M. Le Gars, G. Shukarev, D. Heerwegh, C. Truyers, A. M. de Groot, J. Stoop, S. Tete, W. Van Damme, I. Leroux-Roels, P.-J. Berghmans, M. Kimmel, P. Van Damme, J. de Hoon, W. Smith, K. E. Stephenson, S. C. De Rosa, K. W. Cohen, M. J. Mcelrath, E. Cormier, G. Scheper, D. H. Barouch, J. Hendriks, F. Struyf, M. Douoguih, J. Van Hoof, H. Schuitemaker, *N. Engl. J. Med.* **2021**, *384*, 1824.

[48] D. Wrapp, N. Wang, K. S. Corbett, J. A. Goldsmith, C.-L. Hsieh, O. Abiona, B. S. Graham, J. S. Mclellan, *Science* **2020**, *367*, 1260.
[49] T. N. Starr, A. J. Greaney, S. K. Hilton, D. Ellis, K. H. D. Crawford, A. S. Dingens, M. J. Navarro, J. E. Bowen, M. A. Tortorici, A. C. Walls, N. P. King, D. Veesler, J. D. Bloom, *Cell* **2020**, *182*, 1295.
[50] X. Zhu, D. Mannar, S. S. Srivastava, A. M. Berezuk, J.-P. Demers, J. W. Saville, K. Leopold, W. Li, D. S. Dimitrov, K. S. Tuttle, S. Zhou, S. Chittori, S. Subramaniam, *PLoS Biol.* **2021**, *19*, e3001237.
[51] C. Laffeber, K. de Koning, R. Kanaar, J. H. G. Lebbink, *J. Mol. Biol.* **2021**, *433*, 167058.
[52] T. N. Starr, A. J. Greaney, A. Addetia, W. W. Hannon, M. C. Choudhary, A. S. Dingens, J. Z. Li, J. D. Bloom, *Science* **2021**, *371*, 850.
[53] R. Copin, A. Baum, E. Wloga, K. E. Pascal, S. Giordano, B. O. Fulton, A. Zhou, N. Negron, K. Lanza, N. Chan, A. Coppola, J. Chiu, M. Ni, Y. Wei, G. S. Atwal, A. R. Hernandez, K. Saotome, Y. Zhou, M. C. Franklin, A. T. Hooper, S. Mccarthy, S. Hamon, J. D. Hamilton, H. M. Staples, K. Alfson, R. Carrion, S. Ali, T. Norton, S. Somersan-Karakaya, S. Sivapalasingam, et al., *Cell* **2021**, *184*, 3949.
[54] Z. Liu, L. A. Vanblargan, L.-M. Bloyet, P. W. Rothlauf, R. E. Chen, S. Stumpf, H. Zhao, J. M. Errico, E. S. Theel, M. J. Liebeskind, B. Alford, W. J. Buchser, A. H. Ellebedy, D. H. Fremont, M. S. Diamond, S. P. J. Whelan, *Cell Host Microbe* **2021**, *29*, 477.
[55] S. Jangra, C. Ye, R. Rathnasinghe, D. Stadlbauer, F. Krammer, V. Simon, L. Martinez-Sobrido, A. García-Sastre, M. Schotsaert, H. Alshammary, A. A. Amoako, M. H. Awawda, K. F. Beach, M. C. Bermúdez-González, R. L. Chernet, L. Q. Eaker, E. D. Ferreri, D. L. Floda, C. R. Gleason, G. Kleiner, D. Jurczyszak, J. C. Matthews, W. A. Mendez, L. C. F. Mulder, K. T. Russo, A.-B. T. Salimbangon, M. Saksena, A. S. Shin, L. A. Sominsky, K. Srivastava, *Lancet Microbe* **2021**, *2*, e283.
[56] Q. Li, J. Wu, J. Nie, L. Zhang, H. Hao, S. Liu, C. Zhao, Q. Zhang, H. Liu, L. Nie, H. Qin, M. Wang, Q. Lu, X. Li, Q. Sun, J. Liu, L. Zhang, X. Li, W. Huang, Y. Wang, *Cell* **2020**, *182*, 1284.
[57] A. J. Greaney, T. N. Starr, P. Gilchuk, S. J. Zost, E. Binshtein, A. N. Loes, S. K. Hilton, J. Huddleston, R. Eguia, K. H. D. Crawford, A. S. Dingens, R. S. Nargi, R. E. Sutton, N. Suryadevara, P. W. Rothlauf, Z. Liu, S. P. J. Whelan, R. H. Carnahan, J. E. Crowe, J. D. Bloom, *Cell Host Microbe* **2021**, *29*, 44.
[58] A. Baum, B. O. Fulton, E. Wloga, R. Copin, K. E. Pascal, V. Russo, S. Giordano, K. Lanza, N. Negron, M. Ni, Y. Wei, G. S. Atwal, A. J. Murphy, N. Stahl, G. D. Yancopoulos, C. A. Kyratsous, *Science* **2020**, *369*, 1014.
[59] R. E. Chen, X. Zhang, J. B. Case, E. S. Winkler, Y. Liu, L. A. Vanblargan, J. Liu, J. M. Errico, X. Xie, N. Suryadevara, P. Gilchuk, S. J. Zost, S. Tahan, L. Droit, J. S. Turner, W. Kim, A. J. Schmitz, M. Thapa, D. Wang, A. C. M. Boon, R. M. Presti, J. A. O'halloran, A. H. J. Kim, P. Deepak, D. Pinto, D. H. Fremont, J. E. Crowe, D. Corti, H. W. Virgin, A. H. Ellebedy, et al., *Nat. Med.* **2021**, *27*, 717.
[60] D. Pinto, M. M. Sauer, N. Czudnochowski, J. S. Low, M. A. Tortorici, M. P. Housley, J. Noack, A. C. Walls, J. E. Bowen, B. Guarino, L. E. Rosen, J. Di Iulio, J. Jerak, H. Kaiser, S. Islam, S. Jaconi, N. Sprugasci, K. Culap, R. Abdelnabi, C. Foo, L. Coelmont, I. Bartha, S. Bianchi, C. Silacci-Fregni, J. Bassi, R. Marzi, E. Vetti, A. Cassotta, A. Ceschi, P. Ferrari, et al., *Science* **2021**, *373*, 1109.
[61] M. M. Sauer, M. A. Tortorici, Y.-J. Park, A. C. Walls, L. Homad, O. J. Acton, J. E. Bowen, C. Wang, X. Xiong, W. de van der Schueren, J. Quispe, B. G. Hoffstrom, B.-J. Bosch, A. T. Mcguire, D. Veesler, *Nat. Struct. Mol. Biol.* **2021**, *28*, 478.
[62] C. Wang, R. van Haperen, J. Gutiérrez-Álvarez, W. Li, N. M. A. Okba, I. Albulescu, I. Widjaja, B. van Dieren, R. Fernandez-Delgado, I. Sola, D. L. Hurdiss, O. Daramola, F. Grosveld, F. J. M. van Kuppeveld, B. L. Haagmans, L. Enjuanes, D. Drabek, B.-J. Bosch, *Nat. Commun.* **2021**, *12*, 1715.
[63] G. Song, W.-T. He, S. Callaghan, F. Anzanello, D. Huang, J. Ricketts, J. L. Torres, N. Beutler, L. Peng, S. Vargas, J. Cassell, M. Parren, L. Yang, C. Ignacio, D. M. Smith, J. E. Voss, D. Nemazee, A. B. Ward, T. Rogers, D. R. Burton, R. Andrabi, *Nat. Commun.* **2021**, *12*, 2938.
[64] T. Li, Q. Kan, J. Ge, Z. Wan, M. Yuan, Y. Huang, Q. Xie, Y. Yang, H. Shao, X. Li, L. Ye, A. Qin, Z. Bu, P. Liu, J. Ye, *Cell. Mol. Immunol.* **2021**, *18*, 2563.
[65] K. T. Ng, N. K. Mohd-Ismail, Y.-J. Tan, *Vaccines* **2021**, *9*, 178.
[66] P. Shah, G. A. Canziani, E. P. Carter, I. Chaiken, *Front. Immunol.* **2021**, *12*, 637651.
[67] A. Impagliazzo, F. Milder, H. Kuipers, M. V. Wagner, X. Zhu, R. M. B. Hoffman, R. Van Meersbergen, J. Huizingh, P. Wanningen, J. Verspuij, M. De Man, Z. Ding, A. Apetri, B. Kükrer, E. Sneekes-Vriese, D. Tomkiewicz, N. S. Laursen, P. S. Lee, A. Zakrzewska, L. Dekking, J. Tolboom, L. Tettero, S. Van Meerten, W. Yu, W. Koudstaal, J. Goudsmit, A. B. Ward, W. Meijberg, I. A. Wilson, et al., *Science* **2015**, *349*, 1301.
[68] H. M. Yassine, J. C. Boyington, P. M. Mctamney, C.-J. Wei, M. Kanekiyo, W.-P. Kong, J. R. Gallagher, L. Wang, Y. Zhang, M. G. Joyce, D. Lingwood, S. M. Moin, H. Andersen, Y. Okuno, S. S. Rao, A. K. Harris, P. D. Kwong, J. R. Mascola, G. J. Nabel, B. S. Graham, *Nat. Med.* **2015**, *21*, 1065.
[69] J. S. M. Peiris, K. Y. Yuen, A. D. M. E. Osterhaus, K. Stöhr, *N. Engl. J. Med.* **2003**, *349*, 2431.
[70] A. Zumla, D. S. Hui, S. Perlman, *Lancet* **2015**, *386*, 995.
[71] J. J. Rennick, A. P. R. Johnston, R. G. Parton, *Nat. Nanotechnol.* **2021**, *16*, 266.
[72] P. Sahdev, L. J. Ochyl, J. J. Moon, *Pharm. Res.* **2014**, *31*, 2563.
[73] J. López-Sagaseta, E. Malito, R. Rappuoli, M. J. Bottomley, *Comput. Struct. Biotechnol. J.* **2016**, *14*, 58.
[74] B. N. Fredriksen, J. Grip, *Vaccine* **2012**, *30*, 656.
[75] A. Pachioni-Vasconcelos Jde, et al., *Biomater. Sci.* **2016**, *4*, 205.
[76] L. M. Dunkle, K. L. Kotloff, C. L. Gay, G. Áñez, J. M. Adelglass, A. Q. Barrat Hernández, W. L. Harper, D. M. Duncanson, M. A. Mcarthur, D. F. Florescu, R. S. Mcclelland, V. Garcia-Fragoso, R. A. Riesenberg, D. B. Musante, D. L. Fried, B. E. Safirstein, M. Mckenzie, R. J. Jeanfreau, J. K. Kingsley, J. A. Henderson, D. C. Lane, G. M. Ruíz-Palacios, L. Corey, K. M. Neuzil, R. W. Coombs, A. L. Greninger, J. Hutter, J. A. Ake, K. Smith, W. Woo, et al., *N. Engl. J. Med.* **2022**, *386*, 531.
[77] B. J. Ward, P. Gobeil, A. Séguin, J. Atkins, I. Boulay, P.-Y. Charbonneau, M. Couture, M.-A. D'aoust, J. Dhaliwall, C. Finkle, K. Hager, A. Mahmood, A. Makarkov, M. P. Cheng, S. Pillet, P. Schimke, S. St-Martin, S. Trépanier, N. Landry, *Nat. Med.* **2021**, *27*, 1071.
[78] B. J. Ward, A. Séguin, J. Couillard, S. Trépanier, N. Landry, *Vaccine* **2021**, *39*, 1528.
[79] B. J. Ward, A. Makarkov, A. Séguin, S. Pillet, S. Trépanier, J. Dhaliwall, M. D. Libman, T. Vesikari, N. Landry, *Lancet* **2020**, *396*, 1491.
[80] S. Pillet, P. S. Arunachalam, G. Andreani, N. Golden, J. Fontenot, P. P. Aye, K. Röltgen, G. Lehmicke, P. Gobeil, C. Dubé, S. Trépanier, N. Charland, M.-A. D'aoust, K. Russell-Lodrigue, C. Monjure, R. V. Blair, S. D. Boyd, R. P. Bohm, J. Rappaport, F. Villinger, N. Landry, B. Pulendran, B. J. Ward, *Cell. Mol. Immunol.* **2022**, *19*, 222.
[81] N. C. Dalvie, L. H. Tostanoski, S. A. Rodriguez-Aponte, K. Kaur, S. Bajoria, O. S. Kumru, A. J. Martinot, A. Chandrashekar, K. Mcmahan, N. B. Mercado, J. Yu, A. Chang, V. M. Giffin, F. Nampanya, S. Patel, L. Bowman, C. A. Naranjo, D. Yun, Z. Flinchbaugh, L. Pessaint, R. Brown, J. Velasco, E. Teow, A. Cook, H. Andersen, M. G. Lewis, D. L. Camp, J. M. Silverman, G. S. Nagar, H. D. Rao, et al., *Sci. Adv.* **2022**, *8*, eabl6015.
[82] C. Dong, Y. Wang, G. X. Gonzalez, Y. Ma, Y. Song, S. Wang, S.-M. Kang, R. W. Compans, B.-Z. Wang, *Proc. Nat. Acad. Sci.* **2021**, *118*.

[83] Y. Wang, L. Deng, G. X. Gonzalez, L. Luthra, C. Dong, Y. Ma, J. Zou, S.-M. Kang, B.-Z. Wang, *Adv. Healthcare Mater.* **2020**, *9*, 1901176.
[84] Y. Ma, Y.-Y. Jiao, Y.-Z. Yu, N. Jiang, Y. Hua, X.-J. Zhang, Y.-H. Fu, X.-L. Peng, Y.-P. Zheng, L. Anderson, J.-S. He, *Viruses* **2018**, *10*, 38.
[85] L. Liu, P. Wang, M. S. Nair, J. Yu, M. Rapp, Q. Wang, Y. Luo, J. F.-W. Chan, V. Sahi, A. Figueroa, X. V. Guo, G. Cerutti, J. Bimela, J. Gorman, T. Zhou, Z. Chen, K.-Y. Yuen, P. D. Kwong, J. G. Sodroski, M. T. Yin, Z. Sheng, Y. Huang, L. Shapiro, D. D. Ho, *Nature* **2020**, *584*, 450.